

DAPR: Design Automation for Partially Reconfigurable FPGAs

Shaon Yousuf and Ann Gordon-Ross

NSF Center for High-Performance Reconfigurable Computing (CHREC)

Department of Electrical and Computer Engineering, University of Florida, Gainesville, FL 32611

{yousuf, ann}@chrec.org

Abstract—*Partial reconfiguration (PR) enhances traditional FPGA-based high-performance reconfigurable computing by providing additional benefits such as reduced area and memory requirements, increased performance, and increased functionality. However, since leveraging these additional benefits requires specific designer expertise, which increases design time, PR has not yet gained widespread usage. Even though Xilinx's PR design flow significantly eases PR design, to fully leverage PR benefits designers require extensive PR design flow knowledge, as well as low-level architectural details of the target FPGA device. In this paper, we present a PR design flow and associated tool to automate PR design intricacies and design space exploration. Our design flow and tool can significantly reduce PR design time effort and make PR designs more accessible and amenable to a wider range of PR designers.*

I. INTRODUCTION AND MOTIVATION

Dynamic reconfiguration in SRAM-based FPGAs is an extremely beneficial feature for high-performance embedded designs. By dynamically reconfiguring FPGA *configuration memory* with various design specifications (*bitstreams*), hardware functionality can time-multiplex FPGA resources.

The dynamic reconfiguration method affects the bitstream format. *Full bitstreams*, used for *full reconfiguration* (FR), contain configuration information for the entire FPGA. *Partial bitstreams*, used for *partial reconfiguration* (PR), contain configuration information for a portion of the FPGA. FR and PR expand FPGA resources to nearly an infinite amount, resulting in reduced total resource requirements and increased flexibility through on-demand design specification loading/unloading. Additionally, since FR and PR can potentially decrease the number of required devices or device size, FPGA power consumption can also be reduced [10].

However, dynamic reconfiguration has several drawbacks. Since FR requires reconfiguring the entire FPGA even for small design changes, memory resources are wasted as multiple large full bitstreams containing redundant configuration information need to be stored. Additionally, FR interrupts design execution during FPGA reconfiguration. This interruption or reconfiguration time can impose unacceptable performance overheads, especially for real-time systems. Alternatively, PR mitigates FR's drawbacks by isolating reconfiguration to a portion of the FPGA while all other remaining FPGA resources continue execution [11].

PR designs partition the FPGA into a static region and several individually reconfigurable PR regions (PRRs). The static region implements a PR design's base functionality

and is never reconfigured, while the PRRs are loaded/unloaded on demand with PR modules (PRMs). A PRM constitutes a portion of a PR design's functionality.

Since PR isolates the static region and PRRs, PR reduces memory requirements by eliminating the need for multiple full bitstreams containing redundant configuration information. PR designs require only one full bitstream to initialize a PR design's initial static region and PRRs. During execution, different PRM partial bitstreams can be loaded into the PRRs on demand. Additionally, since partial bitstreams are significantly smaller than full bitstreams, PR reconfiguration time is faster than FR reconfiguration time [9]. PR is particularly useful for designs that do not simultaneously require all their functionality and can benefit from uninterrupted reconfiguration (SDRs [10], JPEG [16]).

Despite PR's enhancements over FR, PR designs have several drawbacks. PR designs are primarily supported by Xilinx's Early-Access (EA) PR design flow [14], which requires manual intervention and significant design time effort. In addition to defining a PR design's functionality and partitioning the design into the PRMs, PR designers must perform PR-specific tasks such as instantiating *bus macro* [14] VHDL specifications. Thus, even with Xilinx's EA PR design flow, realizing PR benefits is challenging as lack of sufficient expertise can result in poor design performance.

Currently, there exists little support for PR designers, and, to the best of our knowledge, there exists no previous efforts to completely automate the EA PR design flow's design space exploration. In this paper we present the Design Automation for Partial Reconfiguration (DAPR) PR design flow. The DAPR design flow reduces PR design time effort and complexity, allowing rapid PR design prototyping and making PR more amenable to a larger range of designers.

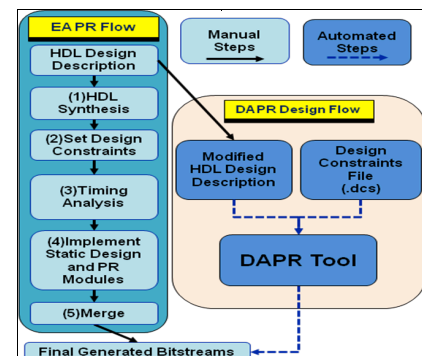


Figure 1: Xilinx's EA PR design flow (left side) and the DAPR design flow (right side).

II. BACKGROUND AND RELATED WORK

A. Xilinx's EA PR Design Flow

Figure 1 (left side) depicts Xilinx's EA PR design flow [14]. The EA PR design flow requires a hierarchical logical partitioning of the VHDL design files into non-overlapping PRMs. Next, the designer must: (1) synthesize each design file separately; (2) create the PR design's floorplan; (3) implement separate non-PR designs for every PRM to PRR combination and perform timing analysis on each design to verify timing requirements; (4) generate place and route information for the static region to create a static design with "holes" (un-placed and un-routed regions) for the PRMs and then generate place and route information for each respective hole's (PRR's) PRM; and (5) merge the static design's place and route information with each PRM's place and route information to generate the PR design's multiple full and partial bitstreams. Each full bitstream contains configuration information for different PRM to PRR combinations allowing any startup PR design functionality and modifying the functionality with partial bitstreams during runtime.

Xilinx ISE [14] utilities individually handle steps 1, 4, and 5 and Xilinx PlanAhead [14] aids step 2 (PR design floorplanning). Floorplanning defines area constraints (set in Xilinx's *user constraints file (.ucf)*) that specify bus macro and resource placements as well as each PRR's location and dimension (size and shape) on the FPGA. Although PlanAhead provides useful floorplanning information, there exists no formal process for determining optimal bus macro and PRR placements. Additionally, FPGA manufacturer provided bus macro placement "best practices" can produce designs with suboptimal design performance [3].

Bus macro floorplanning depends on the target device type. Xilinx Virtex-4 device bus macros are slice-based [14] and span the static region and PRR boundaries. Bus macros are Xilinx provided hardwired logical elements that lock wire routing between the static design and PRMs. All signals except global signals (e.g. clock signals) between the static design and PRMs must pass through bus macros to ensure communication between the static region and PRMs remains established during reconfiguration. PRR floorplanning

ensures PRRs encompass enough hardware resources to support the resource requirements of each PRM mapped to a PRR. Proper floorplanning ensures correct placement of both bus macros and PRRs but several correct placements exist and not all placements will result in the same design performance. For example, a PRR's dimension can affect the maximum attainable clock frequency [5].

Figure 2 (a) depicts a Virtex-4 LX25 FPGA fabric and resource types including: configurable logic blocks (CLBs), block RAMs (BRAMs), first-in first-out buffers (FIFOs), digital signal processors (DSPs), digital clock managers (DCMs), input/output buffers (IOBs), and global buffers (BUFGs). CLBs, BRAMs, FIFOs, and DSPs are in the right and left halves of the fabric, whereas DCMs and BUFGs are in the center. CLBs consist of four slices and are the main logic resource used for sequential and combinatorial circuits.

B. Previous work

Previous work proposes the special-purpose (SP) and multipurpose (MP) [5] PR design methodologies. The SP PR design flow creates custom PR designs tailored for a target system and the MP design flow creates generalized PR design templates for implementing a variety of systems. Since a critical design flow stage is PRR floorplanning, the authors proposed cost functions to evaluate PRR placement quality with respect to the PRR aspect ratio (PRR height in slices divided by PRR width), internal fragmentation, position relative to IOBs, and routability.

Craven et al. [6] presented a high-level development environment for implementing dynamically reconfigurable hardware and used a simulated annealing based automated floorplanner and a *BusMacroHelper* tool for PRR and bus macro placement, respectively. No details were presented on the mechanism or effectiveness of the *BusMacroHelper* tool.

Carver et al. [3] developed an automated simulated annealing-based bus macro placement tool and evaluated the tool using timing results generated by Xilinx's PAR (place and route) utility. However, PRR dimensions were fixed and manually placed and timing evaluation was done for the static and PRM designs separately. Alternatively, DAPR automates PRR placement and evaluates the complete design's timing and partial bitstream size using the final output bitstreams.

Much previous work focuses on floorplanning techniques for reconfigurable designs [1][2][6]. Singhal et al. [13], Cheng et al. [4], and Feng et al. [8] used simulated annealing algorithms for automated PRR floorplanning, but these methods did not automate bus macro placement nor apply their floorplanning techniques to a PR design flow.

Even though there exists much research on bus macro and PRR placement, to the best of our knowledge this is the first attempt to circumvent PR design flow burdens and complexities by automated design space exploration of both bus macro and PRR placement through the evaluation of PR design output bitstreams. Our work also aims to isolate designers from PR design low-level details and intricacies.

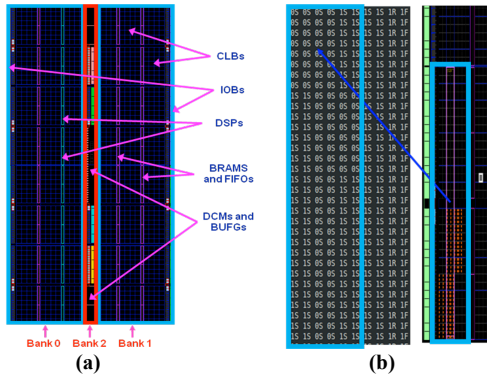


Figure 2: Virtex-4 LX25 (a) Virtex-4 LX25 FPGA resource layout with .dil file banks and (b) .dil to device floorplan mapping.

III. DAPR DESIGN FLOW

The DAPR design flow reduces PR design time effort and complexities by automating many of Xilinx's EA PR design flow's difficult steps. Figure 1 depicts the DAPR design flow (right side) compared to Xilinx's EA PR design flow (left side). The DAPR design flow is a generic, module-based reconfiguration PR design flow and uses vendor specific (Xilinx in this case) utilities to assist in bitstream generation.

The DAPR design flow consists of a manual step and an automated step. In the manual step, the designer annotates the top-level VHDL design files and sets design constraints (optional). These annotations and design constraints serve as input to the automated step, which is orchestrated by the DAPR tool to automate the complex portions of Xilinx's EA PR design flow. The DAPR design flow can be adapted to support different PR devices by updating how the vendor utilities are integrated in the DAPR tool. The DAPR tool works in four phases, which generate the PR design's full and partial bitstreams. In this section, we describe the DAPR design flow steps and the DAPR tool phases.

A. DAPR Design Flow Steps

In the DAPR design flow's first manual step, the designer performs several straightforward tasks to prepare the PR design for the second automated step. First, the designer annotates the VHDL component instantiations in the top-level design file using standard formatted VHDL comments (the designer must also follow Xilinx's EA PR design VHDL formatting guidelines (Section II.A), which assumes that all PRR instantiations are defined in the top-level file). Using VHDL comments ensures that these annotations will not introduce synthesis errors or affect design portability. Optionally, the designer can define PR *design constraints* (e.g. timing, power, area, partial bitstream size, I/O primitive definitions, etc.) and the DAPR tool's effort level control value (Section III.B) in a design constraints file (.dcs).

After completion of the manual step, the DAPR tool's

inputs are the annotated top-level design file, all other design files, and the .dcs file. The DAPR tool manipulates these files to generate the PR design's full and partial bitstreams.

B. DAPR Tool Phases

The DAPR design flow's second automated step, depicted in Figure 3, consists of four phases. In phase 1, information identification uses the design file annotations to identify the static region and PRR instantiations, bus macro instantiations, and design file names. Information extraction extracts port map connection information from the region instantiations. The extracted connection information is written to a PR automation information file (.prai).

Collectively, phases 2 through 4 iteratively generate candidate PR designs. Phase 2, the candidate generation phase, constitutes the bulk of DAPR's work and automatically (1) synthesizes all design files using Xilinx's XST utility, (2) estimates the hardware resource requirements from the generated synthesis log file (.srp) and records the requirements in the .prai file, (3) reads the port map connection information from the .prai file, generates a connectivity information file (.dot), and generates a connectivity graph for these regions, (4) uses the device information library file's (.dil) estimated resources, connectivity information, and .ucf file to build an initial candidate floorplan if the .ucf file does not contain an existing floorplan, otherwise builds a new candidate floorplan, and (5) writes the current candidate floorplan constraints to a new .ucf file. The .dil file is currently generated in-house as part of the DAPR tool and contains the target device's hardware resource information.

Phase 3, the bitstream generation phase, uses the *ngdbuild*, *MAP*, *PAR*, *PR_verifydesign*, and *PR_assemble* utilities (similar to the EA PR design flow's *implement* (4) and *merge* (5) steps) to output the full and partial bitstreams.

Finally, phase 4, the design evaluation phase, determines if the current candidate floorplan meets the specified design constraints. A Perl script estimates the candidate PR design's partial bitstream size, timing, power, and area requirements from the trace report file (.twr), the power report file (.pwr), and the map report file (.mrp) generated by Xilinx's TRACE, XPower, and MAP utilities, respectively. If any design constraints are not met, the DAPR tool returns to phase 2, builds a new unique candidate floorplan, and repeats phases 3 and 4. This iterative process continues until the candidate floorplan meets the design constraints or for a fixed number of successful iterations I_{max} . Successful iterations generate valid candidate PR designs, while unsuccessful iterations fail the place and route step. To bound design exploration time to a reasonable amount, I_{max} is initially set to 100 since experiments showed that a single small design iteration required 15 minutes on average (the Xilinx utilities constituted the majority of this time). However, I_{max} 's value can be specified in the .dcs file.

On phase 4's completion, the DAPR tool outputs the PR design that meets the clock frequency constraint or the PR

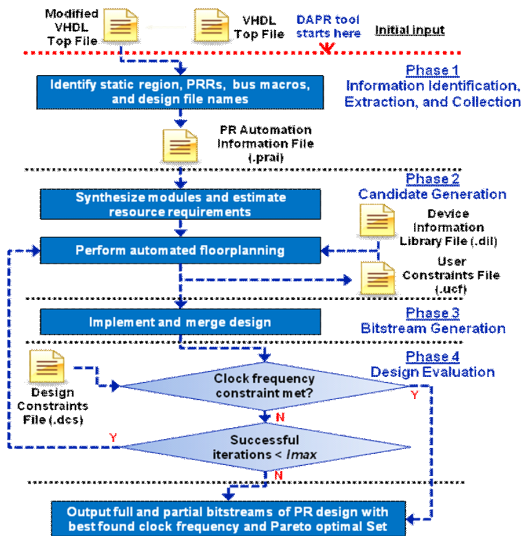


Figure 3: DAPR tool phases.

design with the maximum attainable clock frequency if the clock frequency constraint is not met. The DAPR tool also outputs a Pareto optimal set of PR designs that trade off clock frequency and partial bitstream size.

IV. DAPR TOOL DETAILS

Since the candidate generation phase does most of DAPR's work, in this section we elaborate on this phase's functionality, including .dil file layout and usage in candidate floorplan generation.

A. Device Information Library

The .dil file is primarily used in conjunction with the DAPR tool floorplanner to build candidate floorplans. The .dil file is a two dimensional grid of entries, which specify each FPGA fabric location's resource status and type (e.g. 0S, 0R, 0F, 0D, 0B, 0C). Each entry's X and Y coordinates (grid location) in the .dil file's grid directly translate to the resource's X and Y coordinates on the FPGA fabric. Each entry's numerical and character value indicate the resource's availability (allocated (0) or free (1)) and type (CLB slices (S), BRAMs (R), FIFOs (F), DSPs (D), BUFGs (B), and DCMs (C)), respectively. Figure 2 (b) illustrates an example floorplan built from the Virtex-4 LX25 .dil file.

Each entry's value and corresponding grid location provides an easy method to identify and allocate FPGA resources (currently the DAPR tool includes a .dil file for the Virtex-4 LX 25, but the .dil file could be easily generated for any FPGA device). Resource types can be allocated for a PR design's PRRs, bus macros, or other components (e.g. DCMs, BUFGs) by translating the entry value and grid location into proper .ucf file syntax. The allocation syntax for a PRR is the PRR instance name, as defined in the top level VHDL file, followed by the required resource's type and X and Y coordinates on the FPGA fabric (see [14] for syntax details). To allocate component resources that span across the FPGA fabric (e.g. CLB slices, BRAM, FIFOs, DSPs), the resource range can be specified in the .ucf file. Alternatively, DCM and BUFG allocations do not span the FPGA fabric and must be in the form of single X and Y coordinates. Since defining PRRs that span the center of the device ((a)) is complicated and not recommended [14], we divide the .dil file into three banks (Figure 2 (a)) to isolate resource allocation. Banks 0 and 1 contain CLB slice, BRAM, FIFO, and DSP entries for the FPGA's left and right halves, respectively, and bank 2 contains DCM and BUFG entries.

B. Candidate Floorplan Generation

The DAPR tool floorplanner uses the .dil, .dcs, and .prai files to automatically build candidate design floorplans to determine the *best* PR design (fastest clock frequency) after I_{max} successful iterations. Phase 2's first iteration creates an initial candidate floorplan by placing the PR design's DCMs and BUFGs in the lowest possible free DCM and BUFG X and Y coordinate locations, the PRRs using a *cluster growth (CG) algorithm* [12], and the bus macros randomly around

the PRRs using a *simulated annealing (SA) algorithm* [12]. The candidate floorplan is then used to create a candidate PR design during phases 3 and 4.

Algorithm 1 depicts our CG algorithm which takes as input the set of all PRRs (S), each PRRs maximum resource requirements (R) and port connectivity information (C), the white space (WS) (extra resources), the aspect ratio (AR), total number of PRRs (n), the .dil file, the set of all bus macros (B), the maximum number of bus macros required for each PRR (B_{max}), and the maximum number of successful iterations (I_{max}).

Lines 3-10 use CG to place PRRs where the set of all PRRs S is initially arranged in a linearly ordered list (line 3) using PRR port connectivity information C and a linear ordering algorithm (a widely used technique for building initial placement configurations [12]). The CG algorithm selects PRRs in ascending order from the list (line 7) and selects a placement for the current PRR i (starting at the FPGA's lower left corner and growing diagonally across the device) using the .dil file while minimizing the increase in the cost function (line 8). The cost function attempts to minimize each PRR's placement size, thus minimizing the total number of resources required, while keeping the PRR aspect ratio close to AR . PRR i 's minimum placement size is defined by PRR i 's maximum resource requirements $R(i)$ plus the percentage of extra resources as defined by WS . The default amount of white space allocated is 10% of the maximum resources required by a PRR (WS can be specified in the .dcs file). Additionally, AR defines the placed PRR's shape. AR defaults to 1 if no value is specified.

Lines 11-57 depict our SA-based approach for exploring bus macro placement solutions for B . In order to determine the *initial temperature* T_0 and *initial solution* for the SA algorithm, a random number I_{rand} (between 1 and 10) of successful bus macro placement iterations is performed (lines 11-18) where in each iteration, the set of all bus macros B is placed around the respective PRRs using $bmRnd()$. $bmRnd()$ generates random placement constraints for B , which is written to $BmPlace$ (line 12). $BmPlace$ is written to the .ucf file (line 13) and the corresponding candidate PR design is generated (line 14) and evaluated (line 16). Candidate PR designs are only evaluated if the bitstream generation completes without PAR errors (line 15), otherwise a new candidate floorplan is generated and the current running number of successful iterations I_{curr} remains unchanged (lines 51-52). If five consecutive PAR errors occur, WS is increased by 5% in order to inhibit further PAR errors (lines 55-57). A candidate PR design's clock frequency, partial bitstream size, power, and area requirements are determined and recorded during design evaluation. If the design's clock frequency constraint is met, then *DesignEvaluation()* jumps to line 59, otherwise the average clock frequency change Δ_{avg} (used to compute T_0) for all *uphill* bus macro placements (lower clock frequency PR designs) is determined. The best found bus macro placement constraints

after *Irand* successful iterations is stored in *BmInit* using *clkFq()* (returns the candidate PR design's clock frequency) and is used as the initial solution for SA.

After *Irand* successful iterations complete, the SA algorithm (lines 20-25) sets the current bus macro placement (*BmCurrent*) and the best found bus macro placement (*BmBest*) to *BmInit*, *swp* to *Bmax*, the *acceptance probability* (uphill bus macro placement acceptance probability) *P* to 0.99, the temperature reduction rate λ to 0.85, and the current temperature *T* and the initial temperature T_0 using:

$$T_0 = \frac{\Delta_{avg}}{\ln(P)} \quad (1)$$

Next, for each successful iteration from *Irand* to *Imax* (lines 26-57), the SA algorithm explores new bus macro placements for *B* using a perturbation function (lines 28-33), generates and evaluates the corresponding candidate PR

Input: *S, R, C, WS, AR, n, .dil, B, Bmax, Imax*

Output: Highest clock frequency value, corresponding design number, and floorplan constraints

```

1  Icurr,Uphill,Reject,MT ← 0;
2  Irand ← int(rand(10));
3  S ← LinearOrder(S, C);
4  while Icurr < Imax do
5    DCMBandBUGplacement();
6    for i ← 1 to n do
7      Select PRR i from S;
8      Use R(i), WS, AR and .dil to select PRR i's
       placement with minimum increase in cost function;
9      Write PRM i's placement constraints to ucf file;
10   endfor
11   if Ic < Irand then
12     BmPlace ← bmRnd(B);
13     Write bmInit placement constraints to ucf file;
14     BitstreamGeneration();
15     if PARfail == 0 then
16       DesignEvaluation();
17     if clkFq(bmPlace) > clkFq(bmInit) then
18       BmInit ← BmPlace;
19     if Ic == Irand then
20       BmCurrent ← BmInit;
21       BmBest ← BmInit;
22       swp ← Bmax;
23       P ← 0.99;
24       λ ← 0.85;
25       T ← T0 ← Δavg/ln(P);
26   if Ic ≥ Irand and Ic < Imax then
27     if (Uphill > Bmax or MT > 2*Bmax) then
28       if (swp > 0 and swp ≤ Bmax) then
29         BmNew ← swpRnd(B, swp, Bmax);
30         swp ← swp - I;
31       else
32         BmNew ← bmRnd(B);
33         swp ← Bmax;
34         MT ← MT + 1;
35       Write bmNew placement constraints to ucf file;
36       BitstreamGeneration();
37       if PARfail == 0 then
38         DesignEvaluation();
39       ΔclkFq ← clkFq(BmCurrent) - clkFq(BmNew);
40       if (ΔclkFq < 0 or rand(1) < eΔclkFq/T) then
41         if (ΔclkFq > 0) then
42           Uphill ← Uphill + 1;
43         bmCurrent ← BmNew; (*placement accepted*)
44         if (clkFq(BmCurrent) > clkFq(BmBest)) then
45           BmBest ← BmCurrent;
46         else
47           Reject ← Reject + 1; (*placement rejected*)
48       else
49         T ← λ * T;
50       Uphill,Reject,MT ← 0;
51     if PARfail == 0 then
52       Icurr ← Icurr + 1;
53   else
54     PARerror ← PARerror + 1;
55   if PARerror == 5;
56     WS ← WS + 5;
57     PARerror ← 0;
58   endwhile
59   return clkFqBest(), IBest(), floorplanBest(), Pareto()

```

Algorithm 1: The DAPR tool cluster growth and simulated annealing algorithm for PRR and bus macro placement, respectively.

design (lines 35-38), and accepts or rejects the new placement (lines 39-46) with probability *P* using:

$$P = e^{\frac{\Delta_{avg}}{T}} \quad (2)$$

The perturbation function explores new bus macro placements for *B* (written to *BmNew*) using either *swpRnd()* or *bmRnd()* according to the value of *swp*. If *swp* is greater than 0, *swpRnd()* modifies the current bus macro placements (*BmCurrent*) by performing swaps among existing bus macro placements of each respective PRR while decrementing *swp* each time (line 28-30). If *swp* equals 0, *bmRnd()* performs random bus macro placements while resetting the value of *swp* back to *Bmax* each time (lines 31-33). *swpRnd()* swaps existing bus macro placements for each respective PRR by comparing the current value of *Bmax* and *swp* where, if *swp* ≥ (2*Bmax/3), the input bus macro locations are randomly swapped, if *swp* < (2*Bmax/3) and *swp* > (Bmax/3), the output bus macro locations are randomly swapped, and if *swp* < (Bmax/3) until *swp* equals 0, the input and output bus macro locations are randomly swapped interchangeably. We use this swapping method to provide ample variation in the swapping mechanism, but not too much variation such that the design solution space size is exponential (2^{Bmax}).

After the candidate PR design with the new bus macro placement is generated and evaluated, the change (ΔclkFq) between the new bus macro placement's (*BmNew*) clock frequency from the current bus macro placement's (*BmCurrent*) clock frequency is computed (line 39). If $\Delta\text{clkFq} < 0$ (line 40), the new bus macro placement is not uphill and is accepted as the current bus macro placement (line 43). Also, if the new bus macro placement has the best clock frequency thus far, the new bus macro placement is accepted as the best bus macro placement and is written to *BmBest* (lines 44-45). Alternatively, if the new bus macro placement is uphill, the new solution is accepted with probability *P* and written to *BmCurrent* (line 41). Initially, the acceptance probability *P* is close to 1 during high *T* values, but decreases with decreasing *T*. *T* is decreased in line 49 with the recommended temperature reduction rate $\lambda = 0.85$ [12], if at each given temperature the total number of uphill moves (*Uphill*) or the total number of moves (*MT*) exceeds *Bmax* or 2*Bmax respectively (line 27).

At the end of our algorithm (line 59), the best found clock frequency along with the corresponding iteration number and floorplan is output using *clkFqBest()*, *IBest()*, and *floorplanBest()*, respectively. Also, a Pareto optimal set of PR designs that trade off clock frequency and partial bitstream size are output with *Pareto()*.

V. DAPR DESIGN FLOW EVALUATION

A. Experimental Setup

We implemented the DAPR design flow and tool in the Linux environment. The DAPR tool phases are implemented in Perl scripts for information parsing and file manipulation. The candidate generation phase (2) uses a dot language

interpreter to generate the connectivity graphs. We ran the DAPR tool on a desktop PC with an Intel® Core™ 2 Duo E6750 2.66 GHz CPU and 3.24 GB of RAM and the utilities from Xilinx's ISE version 9.2i04 with PR patch 12 installed.

We evaluated the DAPR design flow SA algorithm with a 32-bit counter core and the complete DAPR design flow with a 1K-point FFT core, a 32-bit CORDIC core, and a 4X4 matrix multiplier (MM) core. We generated the FFT and CORDIC cores using Xilinx's core generation tool and wrote the MM and counter cores in-house. Each PR design's modified HDL design description was taken as input by the DAPR tool and the final bitstreams were generated for the Xilinx ML401 evaluation platform [15] (Virtex-4 LX25 FPGA board). We wrote the original HDL device description for the PR designs with one static region to function as a register to store each PRM's last output and one PRR to load/unload the counter, FFT, CORDIC, or MM core PRMs. In order to maintain feasible simulation times, our PR designs consist of a single PRR due to a significant increase in iteration time for more PRRs (i.e. 50 to 60 minutes per iteration for 2 PRRs). However, we simulated designs with more PRRs and obtained similar results as presented here.

We evaluated our SA algorithm for the 32-bit counter core compared to an exhaustive search (ES) algorithm to find the optimal placement of the input bus macros only (the 32-bit counter has 4 input and output bus macros) and also a random exploration (RE) algorithm of the input bus macros for the largest PRR size (we explored four ascending PRR sizes, which required 24, 120, 360, and 840 iterations, respectively for ES). Although, we obtained similar results for ES by including output bus macros for the smallest PRR size (required 576 iterations), we ran the algorithms for input bus macros only to bound the total DAPR tool run time (e.g. the second smallest PRR size would require 14,400 iterations for ES, which would require 3600 hours or 150 days).

We constructed two test cases for the FFT, CORDIC, and MM PR designs and used the DAPR tool to find the best PR design (fastest clock frequency) within I_{max} successful iterations. For both test cases, we set $I_{max} = 100$. For the first and second test cases, we set $AR=1$ and $AR=10$, respectively, in order to evaluate the aspect ratio's impact on

attainable clock frequency (there is no defined method to predict clock frequency based on PRR aspect ratio [5]) and partial bitstream size. Power and area constraints were not set, which forced the algorithm to place the PRRs with the lowest area (including the extra space) possible. Setting lax power and area constraints allows the PRR placement algorithm to place PRRs with larger areas (extra unused resources), which can reveal higher clock frequencies.

We evaluated our results for the FFT, CORDIC, and MM cores with respect to the highest clock frequency found by the DAPR tool after a fixed number of successful iterations. We did not compare with the optimal clock frequency because our experiments showed that the clock frequency varied unpredictably with different bus macro placements, therefore determining the optimal solution through exhaustive search is impractical given such a large design space. The average runtime to complete 100 iterations on each design was 25 completely automated hours (an acceptable runtime given that a manual process would take several days).

B. Results

We evaluated SA using the percentage of the design space explored (in terms of successful iterations) to achieve the optimal clock frequency obtained from ES. For the smallest PRR size, SA found the optimal solution after exploring 83% of the design space. SA improved on this performance significantly for increasing PRR sizes, finding the optimal solution after exploring only 21.7%, 13.84%, and 18.2% of the design space, respectively. Additionally, for the largest PRR size, SA outperformed RE by requiring 23% less design space exploration.

We evaluated the complete DAPR design flow using the clock frequency and partial bitstream size versus successful iterations. Power requirements were constant in each iteration as each PR design's logic remained constant (no logic reduction was done during synthesis). PRR area requirements did not change significantly during the iterations as PRR size only increased when enough PAR failures occurred and thus was excluded due to lack of space.

Figure 4 depicts the current iteration's clock frequency

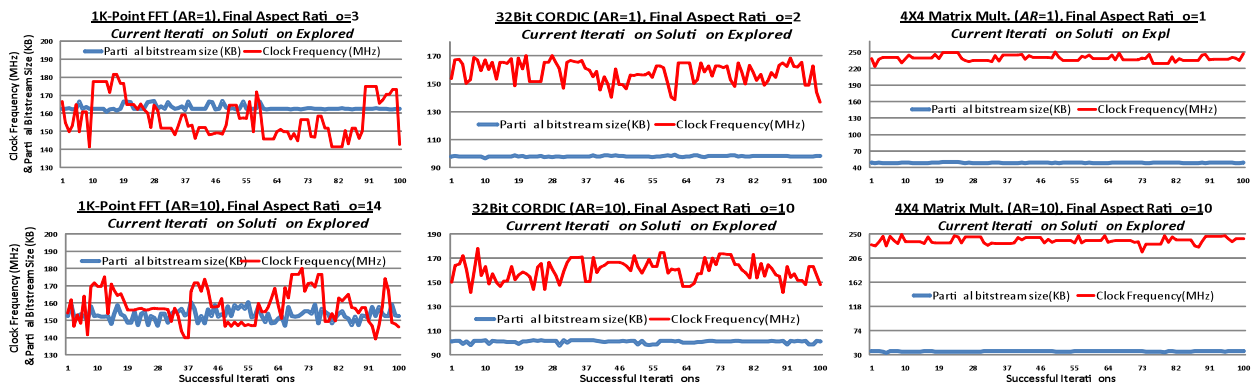


Figure 4: Current iteration's clock frequency and partial bitstream size versus successful iterations with the design's final aspect ratio (top row and bottom row shows designs run with AR=1 and AR=10, respectively).

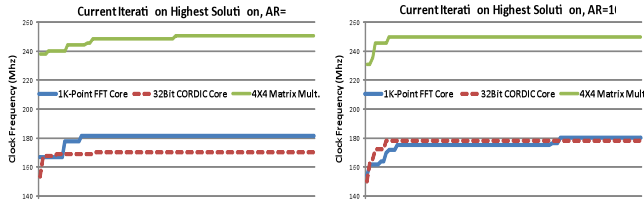


Figure 5: Current iteration's highest Clock Frequency versus successful iterations for designs run with $AR=1$ (left side) and $AR=10$ (right side).

and partial bitstream size versus successful iterations ($AR=1$ top row, $AR=10$ bottom row) and Figure 5 depicts the current highest clock frequency found ($AR=1$ left, $AR=10$ right). Figure 4 tracks the variations in the current iteration's clock frequency and bitstream size while Figure 5 tracks the convergence of the best solution found thus far. Since the AR constraint is not always maintained during design exploration due to variations in the PRR's required resources and the FPGA fabric's resource distribution, the actual (final) AR values of the placed PRR's are noted in the graph titles.

As expected, the results revealed that the greatest improvements in the best solution occur during the first several successful iterations. This growth rate quickly levels off and converges to within 2.31% of the highest achievable solution (within I_{max}) after an average of only 10 iterations. Comparing the convergence rates for different AR values also reveals that higher AR values converge faster than lower AR values requiring on average 28 and 33 iterations, respectively. Additionally, the initial AR value affects the maximum achievable clock frequency. For example, the 32-bit CORDIC core's fastest clock frequency ranged from 170.1 MHz to 178.1 MHz for $AR=1$ and $AR=10$, respectively. The difference in clock frequency arises because large aspect ratios enable our PRR placement algorithm to more easily meet DSP, FIFO, and BRAM requirements with more free resources in each PRR, which reveals additional higher clock frequency routing paths.

Since each candidate PR design results in a different tradeoff between partial bitstream size and clock frequency, the DAPR design flow can also be used to determine the Pareto optimal set of design points, enabling designers to choose the appropriate design tradeoff while examining only a small set of potential designs. Figure 6 shows each candidate design's time period (inverse of the clock frequency) versus partial bit stream size for the 1K-point FFT core with $AR=1$ with the Pareto optimal points highlighted (circular points). For this example, only 3% of the design

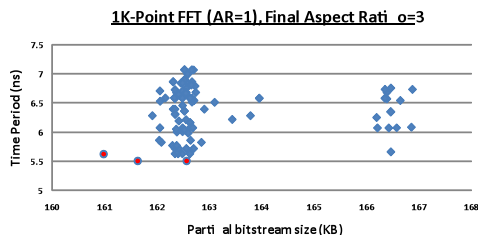


Figure 6: 1K-point FFT ($AR=1$) time period versus partial bitstream size.

space are interesting points, thus significantly reducing the number of designs a designer must consider.

VI. CONCLUSIONS AND FUTURE WORK

In this paper, we present the DAPR design flow, which automates the intricate EA PR design flow steps. DAPR enables designers to specify design constraints and automatically explores the design space using an iterative candidate PR floorplan generation methodology. DAPR outputs the PR design with the fastest clock frequency and a Pareto optimal set of PR design's that trade off clock frequency and partial bitstream size. Therefore, the DAPR flow is highly flexible to meet different designer needs. The DAPR design flow's key contributions include: making PR design more accessible and amenable to a wider range of designers; facilitating rapid design prototyping; and creating high-performance systems with reduced design time effort.

Future work includes investigating techniques to enhance the DAPR tool floorplanning algorithm such as leveraging SA for PRR placement (the CG-based method is unsuitable for heterogeneous floorplanning), efficient use of BUFG and DCM placement, and finding the best design with respect to any design constraint. Support for additional Virtex-4 devices and the ISE design suite 11 is also planned.

VII. ACKNOWLEDGEMENTS

This work was supported in part by the I/UCRC Program of the National Science Foundation under Grant No. EEC-0642422. We gratefully acknowledge tools provided by Xilinx.

VIII. REFERENCES

- [1] P. Banerjee, S. Sur-Kolay and A. Bishnu, "Floorplanning in Modern FPGAs," VLSID, 2007.
- [2] P. Banerjee, M. Sangtani and S. Sur-Kolay, "Floorplanning for Partial Reconfiguration in FPGAs," VLSID, 2009.
- [3] J.M. Carver, R.N. Pittman and A. Forin, "Automatic Bus Macro Placement for Partially Reconfigurable FPGA designs," FPGA 2009.
- [4] L. Cheng and M.D.F. Wong, "Floorplan Design for Multi-million Gate FPGAs," ICCAD, 2004.
- [5] C. Conger, A. D. George and A. Gordon-Ross, "Design Framework for Partial Run-Time FPGA Reconfiguration," ERSAs, 2008.
- [6] S. Craven and P. Athanas, "Dynamic Hardware Development," IJRC, 2008.
- [7] S. Fekete, E. Kohler and J. Teich, "Optimal FPGA module placement with temporal precedence constraints," DATE, 2001.
- [8] Y. Feng, D.P. Mehta, "Heterogeneous floorplanning for FPGAs," VLSID, 2006.
- [9] C. Kao, "Benefits of Partial Reconfiguration," Xcell Journal, 2005.
- [10] E.J. McDonald, "Runtime FPGA partial reconfiguration," IEEE AES Magazine, 2008.
- [11] D. Mesquita, F. Moraes, J. Palma, L. Moller and N. Calazans, "Remote and partial reconfiguration of FPGAs: tools and trends," IPDPS, 2003.
- [12] S. M. Sait and H. Youssef, "VLSI Physical Design Automation: Theory and Practice", World Scientific Publishing Company, 1st edition, 1999.
- [13] L. Singhal and E. Bozorgzadeh, "Multi-layer Floorplanning on a Sequence of Reconfigurable Designs," FPL, 2006.
- [14] Xilinx Inc., "Early Access PR User Guide," UG208, 2006.
- [15] Xilinx Inc., "ML40x Evaluation Platform User Guide," UG080, 2006.
- [16] S. Yousuf and A. Gordon-Ross, "Partial Reconfiguration for Image Processing Applications," MAPLD, 2009.